Published OnlineFirst January 27, 2017; DOI: 10.1158/1541-7786.MCR-16-0301

Genomics

Molecular Cancer Research

# Distinctive Histogenesis and Immunological Microenvironment Based on Transcriptional Profiles of Follicular Dendritic Cell Sarcomas

Maria Antonella Laginestra[1], Claudio Tripodo[2], Claudio Agostinelli[1], Giovanna Motta[3], Sylvia Hartmann[4], Claudia Döring[4], Maura Rossi[1], Federica Melle[3], Maria Rosaria Sapienza[1], Valentina Tabanelli[3], Alessandro Pileri[5], Fabio Fuligni[6], Anna Gazzola[1], Claudia Mannu[1], Carlo Alberto Sagramoso[1], Silvia Lonardi[7], Luisa Lorenzi[7], Francesco Bacci[1], Elena Sabattini[1], Anita Borges[8], Ingrid Simonitsch-Klupp[9], Jose Cabecadas[10], Elias Campo[11], Juan Rosai[12], Martin-Leo Hansmann[4], Fabio Facchetti[7], and Stefano Aldo Pileri[3,13]

## Abstract

Follicular dendritic cell (FDC) sarcomas are rare mesenchymal tumors with variable clinical, morphologic, and phenotypic characteristics. Transcriptome analysis was performed on multiple FDC sarcomas and compared with other mesenchymal tumors, microdissected Castleman FDCs, and normal fibroblasts. Using unsupervised analysis, FDC sarcomas clustered with microdissected FDCs, distinct from other mesenchymal tumors and fibroblasts. The specific endowment of FDC-related gene expression programs in FDC sarcomas emerged by applying a gene signature of differentially expressed genes ($n = 1{,}289$) between microdissected FDCs and fibroblasts. Supervised analysis comparing FDC sarcomas with microdissected FDCs and other mesenchymal tumors identified 370 and 2,927 differentially expressed transcripts, respectively, and on the basis of pathway enrichment analysis ascribed to signal transduction, chromatin organization, and extracellular matrix organization programs. As the transcriptome of FDC sarcomas retained similarity with FDCs, the immune landscape of FDC sarcoma was investigated by applying the CIBERSORT algorithm to FDC sarcomas and non-FDC mesenchymal tumors and demonstrated that FDC sarcomas were enriched in T follicular helper ($T_{FH}$) and T regulatory ($T_{REG}$) cell populations, as confirmed *in situ* by immunohistochemistry. The enrichment in specific T-cell subsets prompted investigating the mRNA expression of the inhibitory immune receptor PD-1 and its ligands PD-L1 and PD-L2, which were found to be significantly upregulated in FDC sarcomas as compared with other mesenchymal tumors, a finding also confirmed *in situ*. Here, it is demonstrated for the first time the transcriptional relationship of FDC sarcomas with nonmalignant FDCs and their distinction from other mesenchymal tumors.

**Implications:** The current study provides evidence of a peculiar immune microenvironment associated with FDC sarcomas that may have clinical utility. *Mol Cancer Res; 15(5); 541–52. ©2017 AACR.*

## Introduction

Follicular dendritic cell (FDC) sarcomas are rare malignancies first described by Monda and colleagues (1), characterized by a rather variable clinical presentation and a high degree of morphologic and immunophenotypical heterogeneity (2). FDC sarcoma presents with lymph node disease in 31% of cases, extranodal disease in 58%, and both nodal and extranodal disease in 10% (3). Cervical nodes are most often affected in nodal presentation. A wide variety of extranodal sites can be affected, most commonly tonsil, gastrointestinal tract, soft tissue, mediastinum, retroperitoneum, omentum, skin, and lung (4). The clinical behavior is generally indolent with nearly 10% of patients dying

[1]Haematopathology Unit, Department of Experimental, Diagnostic and Specialty Medicine (DIMES), S. Orsola-Malpighi Hospital, Bologna University School of Medicine, Bologna, Italy. [2]Tumour Immunology Unit, Department of Health Science, Human Pathology Section University of Palermo School of Medicine, Palermo, Italy. [3]Unit of Diagnostic Haematopathology, European Institute of Oncology, Milan, Italy. [4]Dr. Senckenberg Institute of Pathology, Goethe University, Frankfurt am Main, Germany. [5]Dermatology Unit, Department of Experimental, Diagnostic, and Specialty Medicine (DIMES), S. Orsola-Malpighi Hospital, Bologna University School of Medicine, Bologna, Italy. [6]Genetics and Genome Biology Paediatric Laboratory Medicine (PLM). The Hospital for Sick Children, Toronto, Ontario, Canada. [7]Pathology Unit, Department of Molecular and Translational Medicine, University of Brescia, Brescia, Italy. [8]Histopathology, SRL Diagnostics, Mumbai, India. [9]Institute of Pathology, Medical University of Vienna, Vienna, Austria. [10]Department of Pathology, Portuguese Institute of Oncology, Lisbon, Portugal. [11]Hematopathology Section, Hospital Clinic, IDIBAPS, University of Barcelona, Barcelona, Spain. [12]Centro Diagnostico Italiano, Milano, Italy. [13]Department of Experimental, Diagnostic, and Specialty Medicine (DIMES), Bologna University School of Medicine, Bologna, Italy.

**Note:** Supplementary data for this article are available at Molecular Cancer Research Online (http://mcr.aacrjournals.org/).

M.A. Laginestra and C. Tripodo contributed equally to this study.

**Corresponding Author:** Stefano Aldo Pileri, European Institute of Oncology, Via Ripamonti 435, Milan 20141, Italy. Phone: 39-02-57489521; Fax: 39-02-94379320; E-mail: stefano.pileri@ieo.it/stefano.pileri@unibo.it

**doi:** 10.1158/1541-7786.MCR-16-0301

Published OnlineFirst January 27, 2017; DOI: 10.1158/1541-7786.MCR-16-0301



of the disease; however, local recurrence is frequent (around 40% of cases) and cases displaying an aggressive pace have been reported (5). Moreover, as most studies on this rare entity consist of anecdotal reports, no standard of treatment has been so far identified (6).

An insight into the pathogenesis of FDC sarcomas is definitely lacking. A minority of cases occur in association with the hyaline vascular type of Castleman disease or in the setting of dysregulated immune responses related with Epstein-Barr virus (EBV) infections and inflammatory diseases, such as inflammatory pseudo-tumors, which suggest that FDC hyperplasia may represent a priming condition (7). FDC sarcomas are characterized by the proliferation of spindle-to-oval cells with mild nuclear atypia, which may also comprise epithelioid and/or multinucleated elements (8). Malignant cells usually grow cohesively being aggregated in fascicles and whorls that may be reminiscent of meningioma growth pattern and show a low number of mitotic figures (1–5/10 high-power fields). However, cases with frank cytological atypia, foci of necrosis, and a high mitotic count can be observed, usually corresponding to intra-abdominal masses measuring more than 6 cm and being characterized by a more aggressive clinical course (9). Moreover, a considerable variability is observed in the density and contexture of lymphoid and other immune elements accompanying the malignant proliferation, and no consistent attempt has been so far made in characterizing the FDC sarcoma–associated immune microenvironment (2).

Besides the expression of mesenchymal cell markers, most FDC sarcomas display signs of an FDC immunophenotype with frequent expression of CD21, CD23, CD35, clusterin, Ki-M4P, Claudin 4, and CXCL13 (10). Yet, one or more of such FDC markers can be lost, which may render the differential diagnosis with other sarcomas problematic, warranting testing multiple FDC markers (11). Although a histogenetic affinity to FDC can be argued in these sarcomas based on morphologic and immunophenotypical cues and on the reporting of folliculocentric B lymphocyte–rich morphologic presentations (12), no molecular evidence has been so far provided that could support the preferential representation of FDC transcriptional landscape in comparison with other mesenchymal tumors and highlight the molecular programs characteristic of FDC sarcomas.

In this study, we investigated for the first time the transcriptome of FDC sarcomas and compared it with that of other mesenchymal tumor histotypes.

We demonstrated that on unsupervised cluster analysis, FDC sarcomas are histogenetically linked with FDC and display a peculiar transcriptional profile that significantly diverges from that of other mesenchymal tumors. Moreover, through the application of the CIBERSORT method (13), we could gain insight into the immune microenvironment of FDC sarcomas and highlight a preferential enrichment in the transcriptional programs of follicular helper T cells ($T_{FH}$) and regulatory T cells ($T_{REG}$) lymphoid subsets.

## Materials and Methods

### Case collection

Formalin-fixed and paraffin-embedded tissue (FFPE) samples were selected from the archives of the Pathology Units in Frankfurt, Bologna, Brescia, Bombay, Barcelona, Lisbon, and Vienna. These included 29 surgically resected FDC sarcomas and 32 cases of soft-tissue tumors. Among soft-tissue tumors, histotypes with fibroblastic/myofibroblastic differentiation were selected on the basis of their chance to display transcriptional and phenotypic overlaps with FDC sarcomas, whereas cases with myogenic, adipocytic, chondro-osseous, or neural differentiation were excluded. In details, 3 cases of desmoid-type fibromatosis, 8 cases of dermatofibrosarcoma protuberans, 3 low-grade fibromyxoid sarcomas, 6 inflammatory myofibroblastic tumors (4 $ALK^{+}$, 2 $ALK^{-}$), and 12 solitary fibrous tumors (including 3 cases diagnosed as hemangiopericytomas) were selected. For control purposes, 5 samples of laser microdissected FDCs from regressive germinal centers of HIV-negative hyaline-vascular Castleman disease were adopted. Furthermore, 3 samples of fibroblasts, obtained from routine circumcisions and subsequently FFPE, were included in the gene expression profiling. Samples' characteristics are summarized in Supplementary Table S1.

All FDC sarcoma cases were stained for the FDC markers CD21, CD23, CD35, clusterin, and CXCL13, and diagnoses were confirmed by expert pathologists in a panel session at a multi-head microscope (C. Agostinelli, F. Facchetti, M.-L. Hansmann, S. Hartmann, and S.A. Pileri).

### RNA extraction and gene expression profile generation

RecoverAll Total Nucleic Acid Isolation Kit (Ambion, Life Technologies) was used to extract total RNA from FFPE tissues according to the manufacturer's procedure. RNA was quantified using ND-1000 spectrophotometer running software version 3.0.1 (NanoDrop Technologies, Inc.). After RNA extraction from samples, the Illumina Whole Genome cDNA–mediated Annealing, Selection, extension, and Ligation (DASL) assay was adopted, which allowed for efficient expression profiling of partially degraded RNA from FFPE samples.

In details, the whole-genome DASL assay begins with the conversion of total RNA to cDNA using biotinylated oligo (dT) and random nonamer primers. The biotinylated cDNA is then annealed to the DASL assay pool (DAP) probe groups that contain oligonucleotides specifically designed to interrogate each target sequence in the transcripts. The probes span about 50 bases, making it possible to profile partially degraded RNA. Correctly annealed, assay-specific oligos are subsequently extended and ligated to generate amplifiable products. These templates are labeled during PCR amplification by including fluorescent primers in the reaction. The resulting PCR products are scanned using the BeadArray Reader or iScan System to determine the presence or absence of specific genes (14–17).

### Immunohistochemistry

Immunohistochemistry (IHC) was performed using a polymer-based detection method. Four-micrometers-thick tissue sections were deparaffinized and rehydrated. The antigen unmasking was performed using Epitope Retrieval Solutions (Novocastra) at pH6, pH9, and pH8 in a PT Link Dako pretreatment module at 98°C for 30 minutes. Subsequently, the sections were brought to room temperature and washed in PBS. After neutralization of the endogenous peroxidase with 3% $H_2O_2$ for 10 minutes and Fc blocking by a specific protein block for 8 minutes, the samples were incubated overnight with the monoclonal anti-human PD-1 (Clone NAT105; 1/50 pH8 Abcam 52587), polyclonal anti-human CD274/PDL-1 (1/400 pH9 Acris Antibodies AP 30655PU-N), polyclonal anti-human CD273/PDL-2 (1/400 pH8

Published OnlineFirst January 27, 2017; DOI: 10.1158/1541-7786.MCR-16-0301



Acris Antibodies AP30656PU-N), or monoclonal anti-human Foxp3 (Clone 236A/E7; 1/100 pH9 Abcam 20034) antibodies at 4°C.

Staining was revealed by polymer detection kit (Novolink Polymer Detection System Novocastra) using the substrate chromogen 3,3′-diaminobenzidine (DAB).

IHC for multiple marker detection was performed by 2 sequential rounds of single-marker IHC. In details, the tissue samples were incubated first with the monoclonal anti-human BCL-6 (Clone LN22; 1:100, pH 9, Leica Biosystems Newcastle Ltd.) antibody, with which binding was revealed by polymer detection kit DAB, and secondly, after Fc blocking, with the polyclonal anti-human CD3 (1:100, pH 9, Abcam 5690) antibody revealed by streptavidin-biotin kit (Dako LSAB+ System-AP) using Ferangi Blue chromogen (Biocare Medical Cat. Num. FB813).

All the slides were counterstained with Harris hematoxylin (Novocastra). The sections were analyzed under a Zeiss AXIO Scope A1 optical microscope (Zeiss Oberkochen), and microphotographs were collected using a Zeiss Axiocam 503 Color (Zeiss).

For the comparative analysis of PD-L1 expression among different FDC sarcoma and mesenchymal tumor cases, tissue microarrays (TMA) were constructed, which comprised tumor cell–enriched cores (3 cores per case, 1 mm in diameter) from 22 FDC sarcomas and 27 mesenchymal tumors, which, for control purposes, contained also examples of fibrosarcoma and leiomyosarcoma besides the histotypes object of the transcriptional analysis. TMA slides were evaluated in a blinded fashion by 2 experienced pathologists (F. Fuligni and L. Lorenzi) according to an *ad-hoc* score combining the percentage of positive tumor cells and the intensity of the staining detailed in the Supplementary File.

### Data analysis

The raw data were uploaded in BRB-Array Tools (Version 4.4.1; ref. 18) for normalization and supervised analysis. Unsupervised analyses by hierarchical clustering, principal component analysis (PCA), and non-negative matrix factorization (NMF) algorithms were carried out using MeV v4.7.4 (19) and were applied to identify a group of cases from pathologically defined entities.

To extend the comparison of FDC sarcoma transcriptional programs with a normal mesenchymal cell counterpart other than fibroblasts, we included a published gene expression profile dataset (20) of mesenchymal stem cells (MSC) GSE28205 (GSM698427, GSM698433, GSM698437, GSM698439) for unsupervised hierarchical clustering analysis. In these analyses, the combat method was used to correct batch effects on expression values and to reduce the variability across different microarray experiments (21).

Supervised analyses with SAM (22) and gene set enrichment analysis (GSEA software; ref. 23) were used to identify genes and pathways/signatures associated with FDC sarcoma.

ConsensusPathDB–human interaction database (http://www.consensuspathdb.org; ref. 24) was used to define pathway and functional categories for a gene list annotation.

EASE software was applied to establish the biologic processes of gene signatures differentiating FDC sarcomas from microdissected FDCs and non-FDC mesenchymal tumors, defined according to gene ontology (25–27).

To investigate the infiltrating immune cell landscape of FDC sarcomas and compare it with that of other mesenchymal tumors, we applied CIBERSORT computational method to the gene expression profile data, which accurately quantifies the relative levels of distinct cell types within a complex gene expression mixture. The raw intensity values of our samples (defined as mixture file) were compared to LM22 gene signature file consisting of 547 genes that distinguish 22 mature human hematopoietic populations [T-cell susbets, naïve and memory B cells, plasma cells, natural killer (NK) cells, and myeloid cell subsets] supplied by CIBERSORT tool. The following metrics were adopted: quantile normalization, permutations parameter $= 1{,}000$, $P \leq 0.05$ threshold of the deconvolution across all cell subsets (13).

The Student $t$ test was used on normalized and $\log_2$-transformed intensity value to evaluate the different mRNA expression levels of PD-1, PD-L1, and PD-L2 in FDC sarcomas and other mesenchymal tumors.

The microarray data have been deposited in NCBI's Gene Expression Omnibus (GEO) and are accessible through GEO series accession number GSE90592. More data analysis details and any associated reference are available in the Supplementary File.

## Results

### FDC sarcomas have a distinct FDC-related transcriptional profile which allows differentiation from other mesenchymal tumors

We first adopted an unsupervised hierarchical clustering approach to determine whether the transcriptional profile of the 29 FDC sarcomas had significant overlap with that of other mesenchymal tumors, which encompassed 3 cases of desmoid-type fibromatosis, 8 cases of dermatofibrosarcoma protuberans, 3 low-grade fibromyxoid sarcomas, 6 inflammatory myofibroblastic tumors (4 $ALK^+$, 2 $ALK^-$), and 12 solitary fibrous tumors (including 3 cases diagnosed as hemangiopericytomas).

Within the same unsupervised clustering analysis, we assessed the relationship among the transcriptional profile of FDC sarcomas and that of microdissected FDCs from 5 Castleman disease cases and 3 FFPE fibroblast samples. FDC sarcoma sample profiles clustered together with those of microdissected Castleman FDCs and separately from those of other mesenchymal tumors, which clustered together with fibroblast profiles (Fig. 1A).

Three-dimension PCA revealed that FDC sarcoma cases formed a distinct cloud from other mesenchymal tumors, the percentage of variance explained by the main 3 components being 42.6% (Fig. 1B).

To assess the stability of hierarchical clustering, NMF was run by the use of different number of clusters (range, 2–8) and the optimum number of clusters was determined for $k = 2$ and cophenetic coefficient = 0.991. Two major clusters (one including FDC sarcomas and microdissected Castleman FDCs and the other including non-FDC mesenchymal tumors and fibroblast samples) generated by hierarchical clustering algorithm were confirmed also using NMF method (Supplementary Fig. S1).

These results suggested that FDC sarcoma transcriptional profile was different from that of other mesenchymal neoplasms being correlated with that of FDCs.

Published OnlineFirst January 27, 2017; DOI: 10.1158/1541-7786.MCR-16-0301



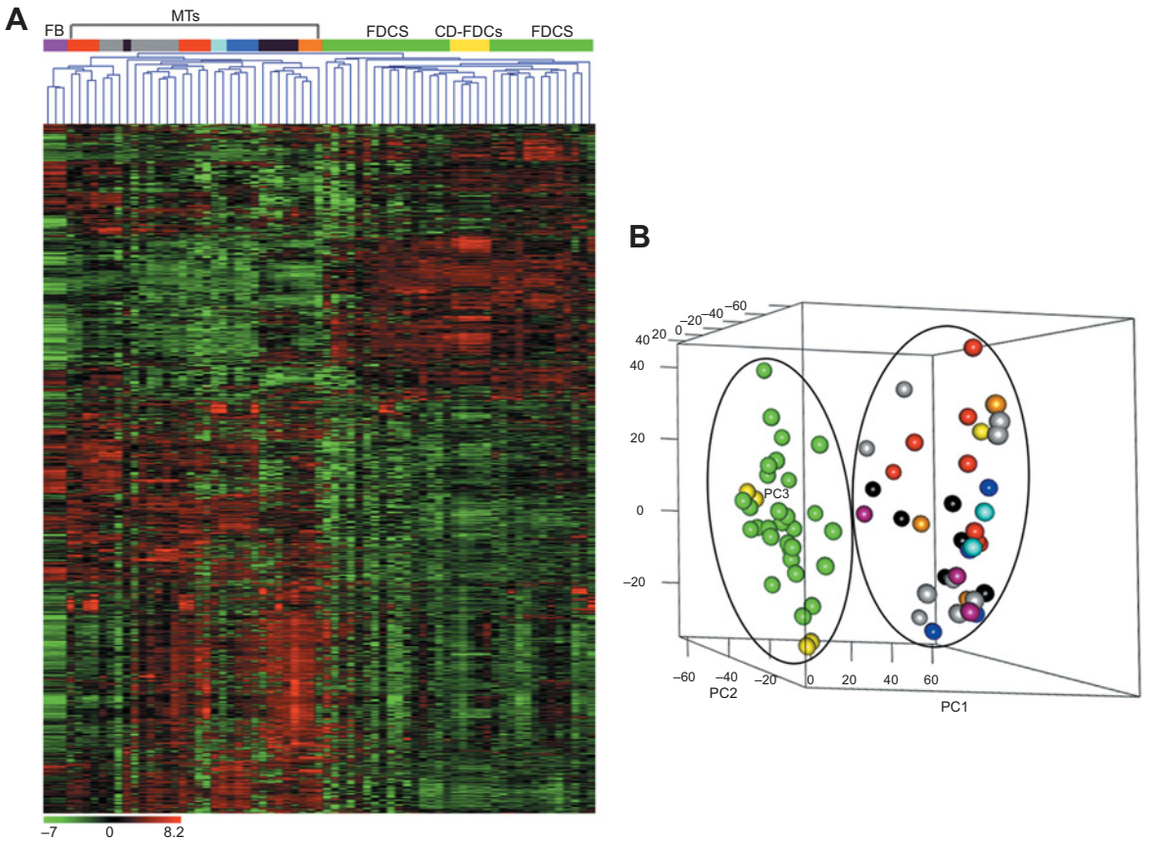


**Figure 1.**

Unsupervised analysis (1,683 genes). **A,** Hierarchical clustering comparing FDC sarcomas, microdissected Castleman FDCs, other mesenchymal sarcomas, and fibroblasts. In the matrix, each row represents a gene and each column represents a sample. The color scale illustrates the relative expression level of a gene across all samples: red represents an expression level above the mean and green represents expression lower than the mean. **B,** PCA plot shows to which extent the different biologic samples group together. In particular, the percentage of variance explained by the 3 main components was 42.65% (component 1, *x*-axis: 25.36%; component 2, *y*-axis: 11.56%; and component 3, *z*-axis: 5.73%). FDC sarcomas (FDCS), green; microdissected Castleman FDCs (CD-FDCs), yellow; fibroblast (FB), purple; other nesenchymal tumors (MTs): desmoid-type fibromatosis (DF), blue; dermatofibrosarcomas protuberans (DFSP), red; fibromyxoid sarcomas (FMS), sky blue, inflammatory myofibroblastic tumors (IM ALK$^+$ and IM ALK$^-$), black; solitary fibrous tumors (SF), gray, hemangiopericytomas (HP), orange.

To evaluate whether significant transcriptional heterogeneity could be detected among the 29 FDC sarcoma samples, we performed unsupervised hierarchical clustering analysis, which identified 2 major groups (Supplementary Fig. S2A). When these 2 groups were compared by applying SAM supervised analysis [false discovery rate (FDR) < 0.01, fold change (FC) $\geq$ 2], only 20 genes were found to be differentially expressed, indicating a low degree of transcriptional heterogeneity within the FDC sarcoma group (Supplementary Fig. S2B). To further verify that the divergences in the transcriptional profile of FDC sarcomas and non-FDC mesenchymal tumors were dictated by the representation of FDC-related transcriptional programs rather than stemming from the heterogeneity in tumor localization and overall environment, we compared the transcriptional profiles of microdissected FDCs with that of fibroblast samples by supervised analysis and adopted the differentially expressed gene signature to perform an unsupervised hierarchical clustering of FDC sarcomas and other mesenchymal tumors. SAM algorithm (FDR $\leq$ 0.001, FC $\geq$ 2) identified neatly separated profiles of microdissected FDCs and fibroblast samples, with 1,289 genes differentially expressed (777 genes upregulated and 512 genes downregulated in FDCs; Supplementary Fig. S3 and Table S2).

When such a signature was applied to FDC sarcomas and non-FDC mesenchymal tumors by hierarchical clustering approach, the FDC sarcomas were robustly separated from other mesenchymal tumor samples (Fig. 2A). Consistently, GSEA revealed a significant enrichment in the genes differentially modulated between microdissected FDCs and fibroblasts in the FDC sarcomas cohort ($P < 0.00001$, Fig. 2B).

As sarcomas generally derive from mesenchymal precursor/stem cells, to further confirm the specific transcriptional relationship between the FDC sarcomas and microdissected FDCs, unsupervised hierarchical clustering analysis was performed including *in silico* profiles of MSCs. We observed that MSCs cluster separately from FDCs and FDC sarcomas, closely to normal fibroblasts and sharing transcriptional features with fibroblasts and non-FDC mesenchymal tumors (Supplementary Fig. S4). This further supports our hypothesis that FDC sarcoma signature differs from the one of neoplastic mesenchymal cells as well as from that of normal mesenchymal cells, at both the stem cell level and terminal step of differentiation.

Published OnlineFirst January 27, 2017; DOI: 10.1158/1541-7786.MCR-16-0301



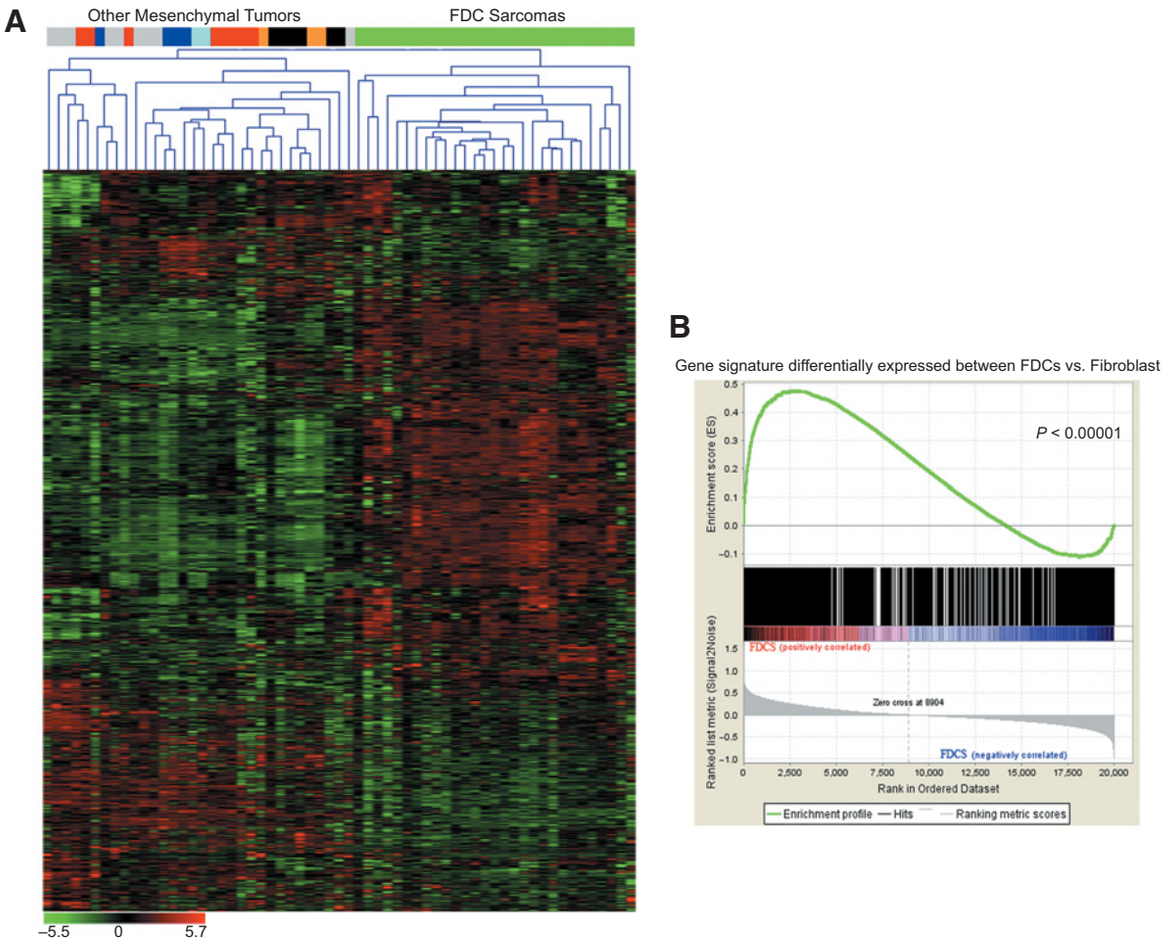


**Figure 2.**

Differentially expressed gene signature (1,289 genes) between microdissected FDCs and fibroblast samples was applied to FDC sarcomas and other mesenchymal tumors by (**A**) hierarchical clustering algorithm that demonstrated a distinct cluster of FDC sarcomas from other mesenchymal tumors. In the matrix, each row represents a gene and each column represents a sample. The color scale illustrates the relative expression level of a gene across all samples: red represents an expression level above the mean and green represents expression lower than the mean. **B,** GSEA revealed significant enrichment of genes up- or downregulated in microdissected FDCs respect to fibroblast in FDC sarcoma. The enrichment score curve was obtained from GSEA software. In the enrichment plot, the *x*-axis shows the rank order of genes from the most upregulated to the most downregulated between microdissected FDC and fibroblast samples. Vertical black line indicates the position of the enriched genes (Hit) comprising the gene set. The graph on the bottom shows the ranked list metric (signal-to-noise ratio) for each gene as a function of the rank in the ordered dataset.

These results indicate that the transcriptional profile of FDC sarcomas, which differs from that of other mesenchymal tumor histotypes, is contributed by FDC-related programs over mesenchymal cell ones.

**The transcriptome of FDC sarcomas is characterized by the deregulation of signal transduction and cell cycle, chromatin organization, extracellular matrix organization, and metabolism pathways.**

On the basis of the demonstration that FDC sarcomas displayed a transcriptional profile distinct from that of other mesenchymal tumors, we focused on analyzing the pathways that were differentially represented in FDC sarcomas in comparison with microdissected Castleman FDCs and with non-FDC mesenchymal tumors, which were likely to reflect the core deregulated programs of these rare malignancies.

On SAM supervised analysis (FDR < 0.1, FC $\geq$ 2), 370 genes distinguished FDC sarcomas from microdissected FDCs (Supplementary Fig. S5A). Of these genes, 64 were significantly upregulated in FDC sarcomas whereas the remaining 306 were downregulated (Supplementary Table S3). When pathway enrichment analysis was performed on differentially expressed genes between FDC sarcomas and microdissected FDCs by the ConsensusPathDB (Reactome pathway data sets, *P* value cutoff = 0.0001), the most represented pathways were those of *signal transduction* and *cell cycle, chromatin organization*, and *metabolism* (Supplementary Table S4). Moreover, a significant enrichment also emerged in genes belonging to the immune system pathway even if the comparison between FDC sarcomas and microdissected Castleman FDCs implied a potentially different contribution of infiltrating immune elements in the 2 sample groups.

Published OnlineFirst January 27, 2017; DOI: 10.1158/1541-7786.MCR-16-0301



Following the identification of the transcriptional pathways modulated between FDC sarcomas and microdissected FDCs, a detailed analysis of the genes contributing to each pathway was performed to assess whether the differentially represented pathways were contributed by genes with high degree of overlap among the different pathways or whether groups of genes specific for each pathway could be identified. Among the differentially expressed genes contributing to the enriched pathways, 85 proved to be selectively involved in one single pathway (Fig. 3A), which substantiated that the deregulation of the above mentioned molecular programs was rather specific being not ascribable to genes with high redundancy among

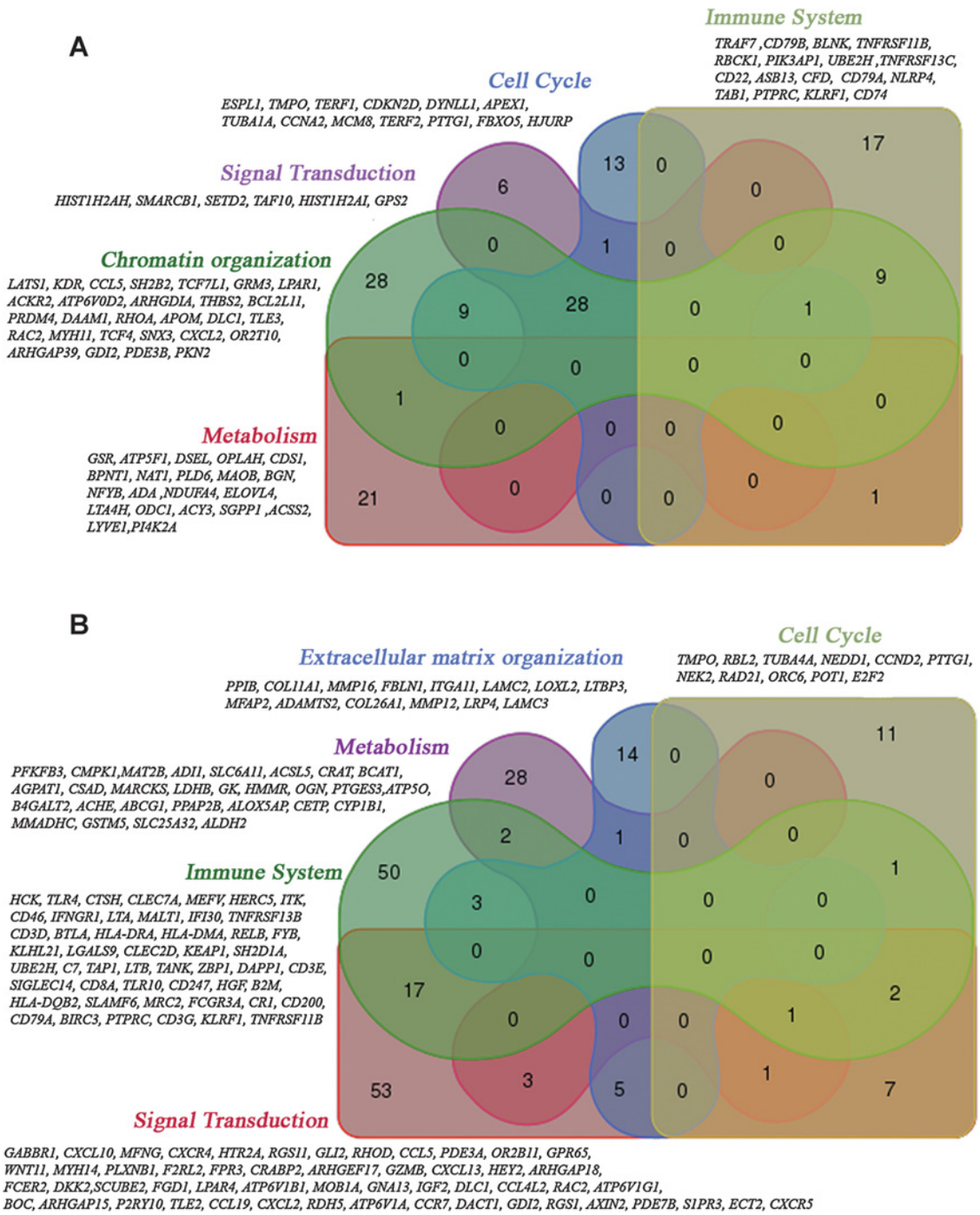


**Figure 3.**

Venn diagrams of the 5 most represented pathways to define unique genes in the 2 different signatures. **A,** Eighty-five genes contributing to each pathway modulated in FDC sarcomas versus microdissected FDCs. **B,** A total of 156 genes contributing to each pathway modulated in FDC sarcomas versus other mesenchymal tumors.

Published OnlineFirst January 27, 2017; DOI: 10.1158/1541-7786.MCR-16-0301



different programs. Of note, among the significantly downregulated genes between FDC sarcomas and microdissected FDCs were included genes reported to be target of loss-of-function mutations on targeted genomic sequencing (28), which belonged to the NF-κB and cell-cycle regulatory pathways (Supplementary Table S5).

We subsequently focused on the 2,927 differentially expressed transcripts between FDC sarcomas and other mesenchymal sarcomas (2,041 upregulated and 886 downregulated in FDC sarcomas) by the SAM analysis (FDR < 0.0001, FC $\geq$ 2; Supplementary Fig. S5B and Table S6) and investigated the differentially regulated transcriptional pathways (Reactome pathway data sets, *P* value cutoff = 0.0001). The programs that were differentially represented in FDC sarcomas in comparison with other mesenchymal tumors were those related to *signal transduction*, *cell cycle*, *metabolism*, *extracellular matrix organization*, and *immune system* (Supplementary Table S7). As for the pathways differentially regulated between FDC sarcomas and microdissected FDCs, those emerging from the comparison of the transcriptional profiles of FDC sarcomas and other mesenchymal tumors featured 156 differentially expressed genes that were selectively involved in one single pathway, further substantiating the specificity of such deregulated programs in FDC sarcomas (Fig. 3B). Indeed, the modulated pathways emerging from the comparison between FDC sarcomas and microdissected FDCs largely overlapped with those differentially modulated between FDC sarcomas and non-FDC mesenchymal tumors, with *chromatin remodeling* and *extracellular matrix organization* pathways resulting selectively involved in the former and in the latter differentiation, respectively. Consistently, 116 genes were shared by the signatures differentiating FDC sarcomas from microdissected FDCs and non-FDC mesenchymal tumors. We then applied EASE software to establish whether specific biologic processes, defined according to Gene Ontology database, were significantly represented among these 116 genes. We found that, for the most part, they corresponded to biologic processes such as chromatin assembly/disassembly, cell growth and maintenance, intracellular signaling cascade, CDK activity, and cell proliferation (Supplementary Table S8).

Overall, these results identify the gene sets and the relative molecular pathways discriminating FDC sarcomas from nonmalignant FDCs and from other mesenchymal tumors and provide new insight into FDC sarcoma pathobiology.

### The immune landscape of FDC sarcomas is skewed toward $T_{FH}$ and $T_{REG}$ enrichment and endowed with PD-1 and PD-L1/2 axis expression

FDCs have a prime role in the mesenchymal organization of the germinal center, which represents a highly dynamic microenvironment where specialized immune cell subsets including B cells, $T_{FH}$, $T_{REG}$, macrophages, and myeloid dendritic cells undertake interactions toward antibody affinity maturation (29). As we demonstrated that the transcriptional profile of FDC sarcomas retained congruity with that of FDCs while clearly differentiating from that of fibroblasts and non-FDC mesenchymal tumors, we investigated the infiltrating immune cell landscape of FDC sarcomas and compared it with that of other mesenchymal tumors in the attempt to identify clues about the enrichment in specific immune cell populations. To this end, we applied the CIBERSORT analysis method to the gene expression profiles of FDC sarcomas and non-FDC mesenchymal tumors, which allowed a detailed enumeration of immune cell subsets from the transcriptional

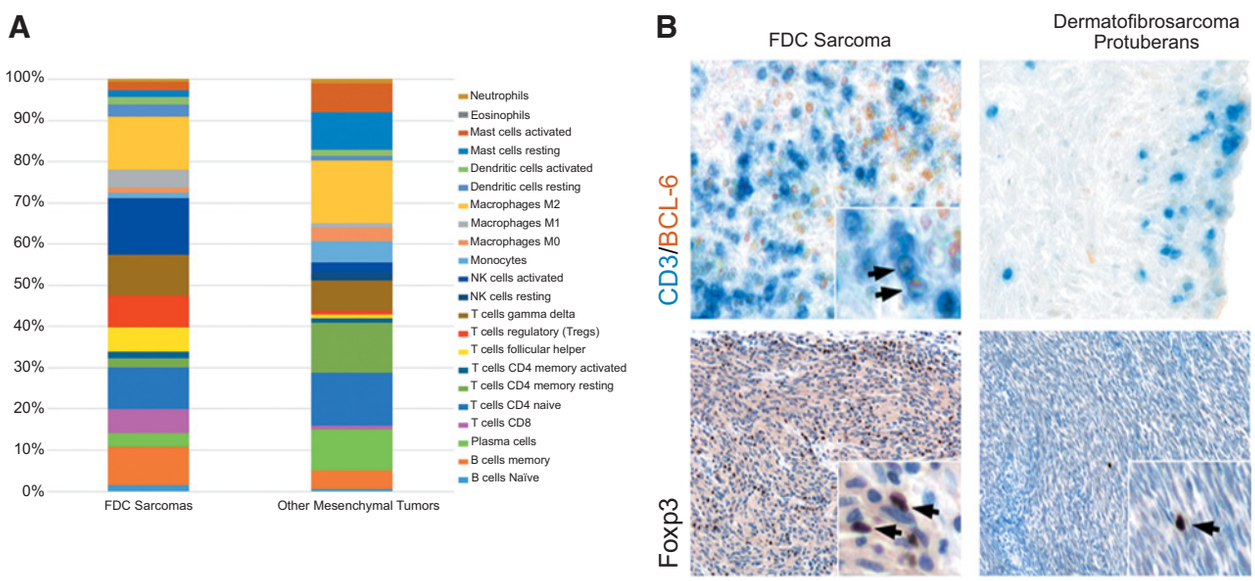


**Figure 4.**

Immune cell landscape of FDC sarcomas compared with other mesenchymal tumors. **A,** CIBERSORT analysis identified a detailed enumeration of immune cell subsets from the gene expression profile. A different profile of immune cells with a significant enrichment of $T_{FH}$, $T_{REG}$, cytotoxic T cells (T cells CD8), NK cells activated population in FDC sarcoma, and plasma cells in the other mesenchymal tumor histotypes. **B,** Representative immunostainings showing the different frequency of CD3 (top, blue signal) and BCL-6 (top, brown signal) expressing bona fide $T_{FH}$ cells in an FDC sarcoma and in a dermatofibrosarcoma protuberans case. A similar difference is shown for the density of Foxp3 (bottom) expressing $T_{REG}$ cells in the 2 cases.

Published OnlineFirst January 27, 2017; DOI: 10.1158/1541-7786.MCR-16-0301



profiles. On CIBERSORT analysis, a different profile of immune cell populations emerged between FDC sarcomas and other mesenchymal tumors (Fig. 4A). Notably, FDC sarcomas proved to be significantly enriched in $T_{FH}$ and $T_{REG}$, 2 populations functionally related with the germinal center microenvironment, and the actual presence of $T_{FH}$ and $T_{REG}$ cells within FDC sarcoma samples was also confirmed *in situ* by IHC analysis for BCL6/CD3 and Foxp3 (Fig. 4B). CIBERSORT analysis highlighted significant differences also in terms of cytotoxic T cells and NK cells that was enriched in FDC sarcoma samples and of plasma cells, which were more represented within the other mesenchymal tumor histotypes.

The consistent enrichment in specific T-cell subsets prompted us to investigate the mRNA expression level of the inhibitory immune checkpoint molecule PD-1 and of its ligands PD-L1 and PD-L2 that constitute a pivotal axis in the regulation of adaptive antitumor immunity within the tumor microenvironment (30). The inhibitory checkpoint receptor PD-1 is expressed on activated effector T and NK cells as a regulatory feedback inducing their functional exhaustion and represents a phenotypic marker of $T_{FH}$ and $T_{REG}$ cells correlated with the activation status (31–33). In keeping with a higher frequency of infiltrating $T_{FH}$, $T_{REG}$, and cytotoxic elements, PD-1 mRNA expression levels proved to be significantly higher in FDC sarcoma samples than in the other mesenchymal tumors tested ($P = 0.013$; Fig. 5A), and the same trend was observed for the PD-L1 and PD-L2 ligands ($P = 0.00024$, $P = 0.00019$, respectively; Fig. 5B and C). The presence of PD-1–expressing tumor-infiltrating lymphocytes in FDC sarcomas was detected *in situ* by IHC as well as the expression of PD-L1 and PD-L2 by malignant elements and infiltrating immune cells (Fig. 5D). Within the FDC sarcoma group, we also investigated the correlation between the expression of PD-1 and the frequency of cytotoxic T cells, $T_{FH}$, $T_{REG}$, and NK cells, as determined by CIBERSORT analysis, to assess whether one or more of these cell subsets could be identified as predominant determinant(s) of PD-1 expression levels. No significant correlation was identified between PD-1 mRNA expression levels and the frequency of any of the differentially enriched cell populations (not shown), which implicated the contribution of diversified tumor-infiltrating lymphocyte populations to PD-1 mRNA expression within the FDC sarcoma microenvironment. Moreover, no significant correlation could be identified between PD-1 mRNA expression levels and those of the PD-1 ligands (not shown), possibly owing to the higher variation of PD-1 expression as compared with that of the ligands among different FDC sarcoma samples and to the puzzling effect of the PD-1 ligand expression in the infiltrating immune cells. Indeed, the consistent expression of PD-1 ligand among the different FDC sarcoma cases also emerged at the protein level by extending IHC analysis on TMAs constructed from 22 FDC sarcoma and 27 mesenchymal tumor samples. Tumor cell–enriched cores from FDC sarcomas showed conspicuous reactivity for PD-L1 in more than 60% of cases whereas cores from other mesenchymal tumors displayed detectable PD-L1 in only 4% of cases (Fig. 5E; Supplementary table S9).

These results indicate that FDC sarcomas have a peculiar immunological microenvironment that is contributed by functionally specialized T-cell populations, namely $T_{FH}$ and $T_{REG}$, and that can fall under the influence of the PD-1 and PD-L1/2 axis.

## Discussion

Along their malignant transformation, mesenchymal cells may display variable signs of differentiation toward one lineage while retaining considerable plasticity (34). The correspondence between the expression or the disruption of specific transcriptional programs and the acquisition or maintenance of a specific functional phenotype has been poorly investigated. FDCs are highly specialized reputed mesenchymal cells which differentiate from perivascular mesenchymal precursors under the driving stimuli of lymphoid tissue inducer cells, lymphotoxins, and other cytokines (35). The acquisition of the FDC phenotype is characterized by the expression of molecules involved in the organization of the peculiar matricellular and adhesive milieu of the germinal center, which includes type-I collagen, SPARC, ICAM-1, VCAM-1, and MAdCAM-1, and finds commonality in presumed mesenchymal elements of other specialized microenvironments such as those of the bone marrow hematopoietic niche (36). Moreover, FDC phenotypic specification is associated with the expression of functional mediators of B-cell chemoattraction (i.e., CXCL-13), tropism (BAFF, IL6), co-stimulation (C4bBP, iC3b/C3dg), and immune complex trapping (CD21, CD35, CD23). In FDC sarcomas, features of the FDC phenotype can be maintained, although clones may present a high degree of heterogeneity as far as the expression of FDC-related markers is concerned (11). We found that sarcomatous transformation of FDCs is characterized by the maintenance of FDC-related transcriptional programs as suggested by the clustering of FDC sarcoma cases with microdissected FDCs and by the successful differentiation of FDC sarcomas from other mesenchymal tumors according to the application of a differential signature obtained from the comparison between FDCs and fibroblasts. This evidence implied that FDC-related programs were prevalent over those resulting from a common reputed mesenchymal origin in defining FDC sarcoma identity. From the attempt to identify the motifs of the transcriptional deregulation occurring in sarcomatous FDCs as compared with their nonmalignant counterpart, we derived evidence of a prevalent downmodulation of transcriptional networks involved in cell-cycle regulation, chromatin organization, and signal transduction, which included transcripts of genes directly involved in or correlated with the FDC sarcoma mutational landscape, such as NF-κB transcriptional targets and cyclin-dependent kinase regulators (28). From these results, the abating of regulatory fringes in key cellular programs rather than the forcing pressure of a specific oncogenic pathway emerges as the transcriptional imprint of FDC malignant phenotype. In the comparison between the gene expression profile of FDC sarcomas and that of other mesenchymal tumors, the same pathways were complemented by extracellular matrix and immune system molecular programs, which underlined the association of FDC clones with a distinct extracellular matrix and immunologic contexture consistent with preserved FDC functional differentiation. On this respect, our findings did not support the dichotomy of FDC sarcomas recently emerged from miRNA profiling (37), suggesting the existence of 2 distinct FDC sarcoma groups closer to fibroblasts/myopericytic tumors and Castleman microdissected FDCs, respectively. Indeed, on transcriptional profiling, all the FDC sarcoma cases clustered together with Castleman disease–microdissected FDCs remaining clearly distinct from fibroblasts

Published OnlineFirst January 27, 2017; DOI: 10.1158/1541-7786.MCR-16-0301



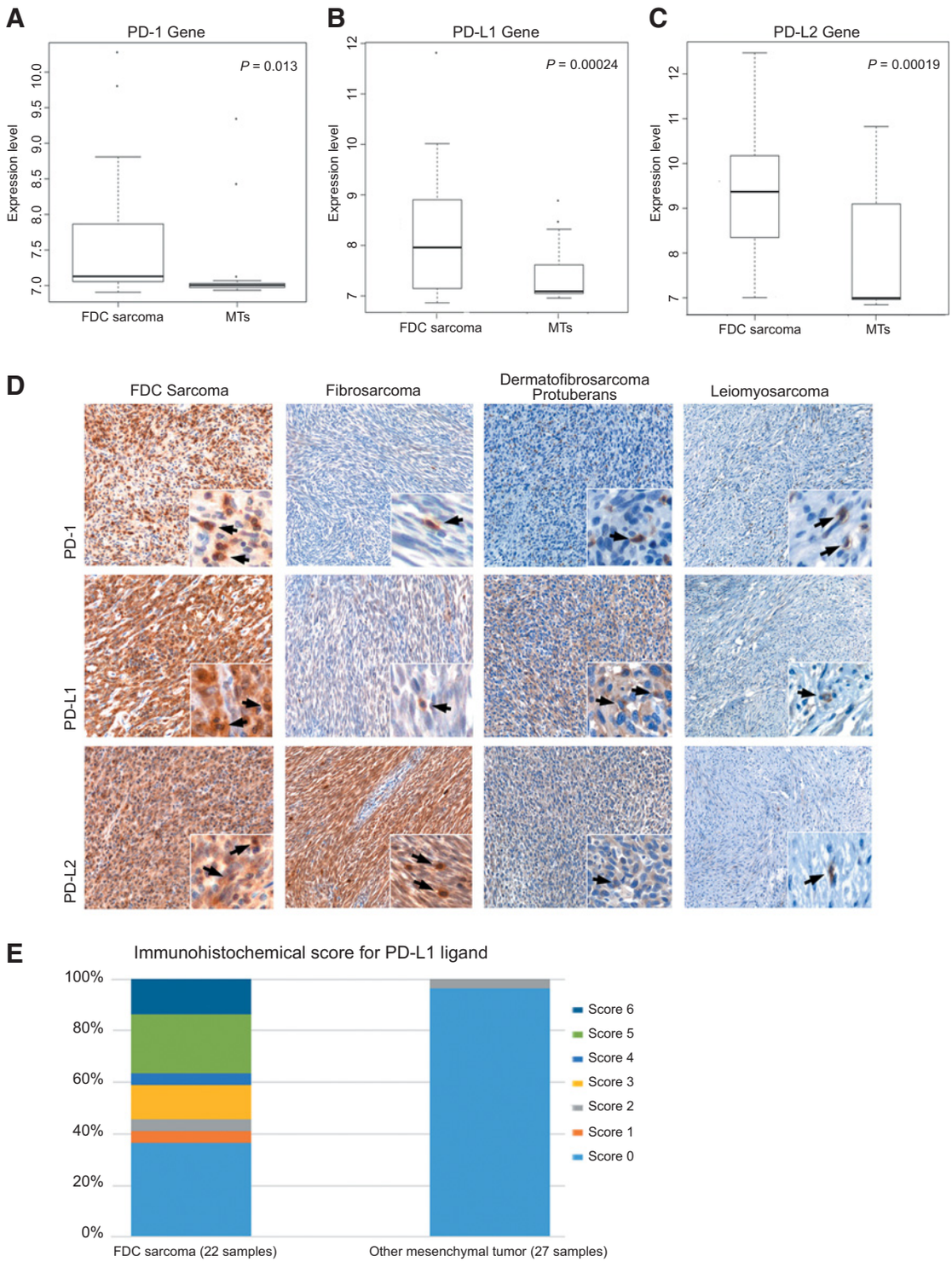


**Figure 5.**

Correlation between PD-1, PD-L1, and PD-L2 mRNA expression levels in FDC sarcoma versus other mesenchymal tumors (MT). Box plot of significant difference of mRNA expression levels (**A**) PD-1, (**B**) PD-L1, and (**C**) PD-L2. **D,** Representative immunostainings showing PD-1 (top) expressing infiltrating immune cells and the conspicuous expression of PD-L1 (middle) and PD-L2 (bottom) ligands in a case of FDC sarcoma, as compared with a control dermatofibrosarcoma protuberans, fibrosarcoma, and leiomyosarcoma cases. **E,** Combined IHC score for PD-L1 ligand in TMAs constructed from 22 FDC sarcoma (FDCS) and 27 mesenchymal tumor samples.

Published OnlineFirst January 27, 2017; DOI: 10.1158/1541-7786.MCR-16-0301



and other mesenchymal tumors and displayed a low degree of transcriptional heterogeneity. This apparent discrepancy should be considered in the light of miRNA and mRNA profiles reflecting different levels of information in cancer. Indeed, miRNA profiles, as expression of regulatory networks tightly linked with cell identity, can be efficiently adopted to infer information related with the cell/tissue of origin even in the case of profoundly depressed functional differentiation, such as in poorly differentiated cancers (38), whereas mRNA profiles are better reflective of the actual differentiation status mirroring the transcriptional activity (39). Because of their function in epigenetic regulation of cell processes, miRNA profiles can therefore display considerable variability among individual cases even in the presence of a rather homogeneous transcriptional profile.

Application of the CIBERSORT method for the enumeration of infiltrating immune cell fractions from gene expression profiles revealed the enrichment in $T_{FH}$ and $T_{REG}$ populations in FDC sarcomas, which was also corroborated by *in situ* IHC analyses. $T_{FH}$ cells are a specialized T-cell subset providing growth and differentiation support to B cells of the germinal center toward the establishment of antibody-mediated immune responses (40). Controlled by the synergic activity of $T_H$ and germinal center–related transcription factors, $T_{FH}$ are essential for the germinal center cellular networking (41), the impairment of their function resulting in defective systemic humoral immunity (42). $T_{FH}$-promoted responses are regulated by follicular regulatory T cell ($T_{FR}$) subsets, which play a fundamental role also in the selection of antigen-specific B cells within the germinal center environment (43). The maintenance of these T-cell populations does not require ongoing germinal center responses, while depending on germinal center microenvironment–associated signals (44). Our finding of a significant enrichment in $T_{FH}$ and $T_{REG}$ cells in FDC sarcoma samples, as compared with other mesenchymal tumors, cope with FDC sarcomas being associated with the remnants of a germinal center–type microenvironment. Among the signals overrepresented in germinal center immune networking is the immunoregulatory PD-1 and PD-L1/2 axis, which controls the function of germinal center T-cell subsets expressing the PD-1 receptor and the survival and differentiation of germinal center B cells expressing PD-L2 (45). According to the higher frequency of germinal center–related T-cell populations in FDC sarcomas, PD-1, as well as its ligands PD-L1 and PD-L2, was significantly higher at mRNA and protein level in FDC sarcomas as compared with other mesenchymal tumor histotypes included in our study (desmoid-type fibromatosis, dermatofibrosarcoma protuberans, low-grade fibromyxoid sarcomas, Inflammatory myofibroblastic, and solitary fibrous tumors). Interestingly, both *CD274* (PD-L1) and *PDCD1LG2* (PD-L2) genes are coded in a 9p24 region which has been reported to undergo copy number gain in FDC sarcomas (28). Within the FDC sarcoma environment, malignant cell PD-L1/2–mediated engagement of PD-1–expressing immune cell subsets can be interpreted in dramatically different ways according to the functional differentiation state of the immune cells involved in the interaction. Indeed, while PD-1 engagement can promote the maintenance and fitness of FDC sarcoma–infiltrating $T_{FH}$ and $T_{REG}$ cells, it may mediate functional exhaustion of effector cells, such as cytotoxic T cells and NK cells. Indeed, besides amplification of the 9p24 region, abundant PD-1 ligand expression in FDC sarcomas may represent the checkpoint for T-cell responses against immunogenic mutant antigens (46). The high expression of PD-L1/2 mRNA in FDC sarcoma cases is likely responsible for the lack of correlation with PD-1 mRNA levels, which displayed a more conspicuous variation. Moreover, we failed to identify specific infiltrating immune cell populations, among those enriched in FDC sarcoma samples, with prominent correlation (in terms of frequency) with PD-1 mRNA expression levels. This could be interpreted in the light of the promiscuous expression of PD-1 by diverse immune cell subsets, such as $T_{FH,}$ $T_{REG,}$ NK cells, which could variably contribute to PD-1 mRNA at discrete phases of their functional activation. These data depicting the immune environment of FDC sarcomas should be considered in the prospect of potential targeted immunotherapies, for example immune checkpoint blockade, despite their inference from molecular profiling. Indeed, they are well matched by recent evidence indicating that response to antibody-based immunotherapies may be observed even in the case of discrepant target detection between protein- and mRNA-based techniques, the latter being purportedly endowed with higher sensitivity (47).

Overall, we demonstrated for the first time the transcriptional relationship of FDC sarcomas with nonmalignant FDCs and identified the molecular programs deregulated in these rare malignancies and allowing their differentiation from other mesenchymal tumors. Furthermore, we provided evidence of a peculiar immunologic microenvironment associated with FDC sarcomatous proliferation and underscored the potential relevance of PD-1 and PD-L1/2 axis in the regulation of FDC sarcoma immune contexture.

## Disclosure of Potential Conflicts of Interest

S.A. Pileri has received speakers bureau honoraria from and is a consultant/advisory board member for Takeda. No potential conflicts of interest were disclosed by the other authors.

## Authors' Contributions

**Conception and design:** M.A. Laginestra, C. Tripodo, A. Pileri, M.L. Hansmann, F. Facchetti, S.A. Pileri

**Development of methodology:** M.A. Laginestra, A. Pileri

**Acquisition of data (provided animals, acquired and managed patients, provided facilities, etc.):** M.A. Laginestra, C. Tripodo, C. Agostinellli, G. Motta, S. Hartmann, M. Rossi, F. Melle, V. Tabanelli, A. Pileri, A. Gazzola, C. Mannu, C.A. Sagramoso, F. Bacci, E. Sabattini, A. Borges, I. Simonitsch-Klupp, J. Cabecadas, E. Campo, M.L. Hansmann, F. Facchetti, S.A. Pileri

**Analysis and interpretation of data (e.g., statistical analysis, biostatistics, computational analysis):** M.A. Laginestra, C. Tripodo, A. Pileri, F. Fuligni, L. Lorenzi, J. Rosai, S.A. Pileri

**Writing, review, and/or revision of the manuscript:** M.A. Laginestra, C. Tripodo, C. Agostinellli, S. Hartmann, M.R. Sapienza, A. Pileri, L. Lorenzi, J. Cabecadas, E. Campo, F. Facchetti, S.A. Pileri

**Administrative, technical, or material support (i.e., reporting or organizing data, constructing databases):** M.A. Laginestra, M. Rossi, A. Pileri, S. Lonardi, I. Simonitsch-Klupp

**Study supervision:** A. Pileri, J. Rosai, M.L. Hansmann, S.A. Pileri

**Other (bioinformatic support):** C. Döring

**Other (histological and immunophenotypical revision and diagnosis confirmation):** F. Facchetti

## Acknowledgments

The authors are grateful to Valentina Indio, Matilde De Luca, and Giuseppe Tarantino for their skilled bioinformatics assistance.

## Grant Support

This work was supported by grants from the Italian Association for Cancer Research (AIRC 5×1000, n. 10007 and AIRC IG, n. 15762 to S.A. Pileri, AIRC IG, n. 15999 to C. Tripodo); Emilia Romagna Region – University Programme 2010–2012: Area 1 "Innovative approaches to the diagnosis and pharmacogenetic-based therapies of primary hepatic tumours, peripheral B- and T-lymphomas and lymphoblastic leukaemias".

The costs of publication of this article were defrayed in part by the payment of page charges. This article must therefore be hereby marked *advertisement* in accordance with 18 U.S.C. Section 1734 solely to indicate this fact.

Received September 5, 2016; revised December 2, 2016; accepted December 15, 2016; published OnlineFirst January 27, 2017.

## References

1. Monda L, Warnke R, Rosai J. A primary lymph node malignancy with features suggestive of dendritic reticulum cell differentiation. A report of 4 cases. Am J Pathol 1986;122:562–72.
2. Swerdlow SH, Campo E, Pileri SA, Harris NL, Stein H, Siebert R, et al. The 2016 revision of the World Health Organization classification of lymphoid neoplasms. Blood 2016;127:2375–90.
3. Saygin C, Uzunaslan D, Ozguroglu M, Senocak M, Tuzuner N. Dendritic cell sarcoma: a pooled analysis including 462 cases with presentation of our case series. Crit Rev Oncol Hematol 2013;88:253–71.
4. Hollowood K, Stamp G, Zouvani I, Fletcher CD. Extranodal follicular dendritic cell sarcoma of the gastrointestinal tract. Morphologic, immunohistochemical and ultrastructural analysis of two cases. Am J Clin Pathol 1995;103:90–7.
5. Chan JK, Fletcher CD, Nayler SJ, Cooper K. Follicular dendritic cell sarcoma. Clinicopathologic analysis of 17 cases suggesting a malignant potential higher than currently recognized. Cancer 1997;79:294–313.
6. Soriano AO, Thompson MA, Admirand JH, Fayad LE, Rodriguez AM, Romaguera JE, et al. Follicular dendritic cell sarcoma: a report of 14 cases and a review of the literature. Am J Hematology 2007;82:725–8.
7. Chan AC, Chan KW, Chan JK, Au WY, Ho WK, Ng WM. Development of follicular dendritic cell sarcoma in hyaline-vascular Castleman's disease of the nasopharynx: tracing its evolution by sequential biopsies. Histopathology 2001;38:510–8.
8. Perez-Ordoñez B, Rosai J. Follicular dendritic cell tumor: review of the entity. Semin Diagn Pathol 1998;15:144–54.
9. Perez-Ordonez B, Erlandson RA, Rosai J. Follicular dendritic cell tumor: report of 13 additional cases of a distinctive entity. Am J Surg Pathol 1996;20:944–55.
10. Vermi W, Lonardi S, Bosisio D, Uguccioni M, Danelon G, Pileri S, et al. Identification of CXCL13 as a new marker for follicular dendritic cell sarcoma. J Pathol 2008;216:356–64.
11. Facchetti F, Lorenzi L. Follicular dendritic cells and related sarcoma. Semin Diagn Pathol 2016;33:262–76.
12. Lorenzi L, Lonardi S, Petrilli G, Tanda F, Bella M, Laurino L, et al. Folliculocentric B-cell-rich follicular dendritic cells sarcoma: a hitherto unreported morphological variant mimicking lymphoproliferative disorders. Hum Pathol 2012;43:209–15.
13. Newman AM, Liu CL, Green MR, Gentles AJ, Feng W, Xu Y, et al. Robust enumeration of cell subsets from tissue expression profiles. Nat Methods 2015;12:453–7.
14. Laginestra MA, Piccaluga PP, Fuligni F, Rossi M, Agostinelli C, Righi S, et al. Pathogenetic and diagnostic significance of microRNA deregulation in peripheral T-cell lymphoma not otherwise specified. Blood Cancer J 2014;4:259.
15. Waddell N, Cocciardi S, Johnson J, Healey S, Marsh A, Riley J, et al. Gene expression profiling of formalin-fixed, paraffin-embedded familial breast tumours using the whole genome-DASL assay. J Pathol 2010;221:452–61.
16. April C, Klotzle B, Royce T, Wickham-Garcia E, Boyaniwsky T, Izzo J, et al. Whole-genome gene expression profiling of formalin-fixed, paraffin-embedded tissue samples. PLoS One 2009;4:e8162.
17. April CS, Fan JB. Gene expression profiling in formalin-fixed, paraffin-embedded tissues using the whole-genome DASL assay. Methods Mol Biol 2011;784:77–98.
18. Simon R, Lam A, Li MC, Ngan M, Menenzes S, Zhao Y. Analysis of gene expression data using BRB-array tools. Cancer Inform 2007;3:11–7.
19. Saeed AI, Sharov V, White J, Li J, Liang W, Bhagabati N, et al. TM4: a free, open-source system for microarray data management and analysis. BioTechniques 2003;34:374–8.
20. Dani N, Olivero M, Mareschi K, van Duist MM, Miretti S, Cuvertino S. , et al. The MET oncogene transforms human primary bone-derived cells into osteosarcomas by targeting committed osteo-progenitors. J Bone Miner Res 2012;27:1322–34
21. Johnson WE, Li C, Rabinovic A. Adjusting batch effects in microarray expression data using empirical Bayes methods. Biostatistics 2007;8:118–27
22. Tusher VG, Tibshirani R, Chu G. Significance analysis of microarrays applied to the ionizing radiation response. Proc Natl Acad Sci U S A 2001;98:5116–21.
23. Subramanian A, Tamayo P, Mootha VK, Mukherjee S, Ebert BL, Gillette MA, et al. Gene set enrichment analysis: a knowledge-based approach for interpreting genome-wide expression profiles. Proc Natl Acad Sci U S A 2005;102:15545–50.
24. Kamburov A, Stelzl U, Lehrach H, Herwig R. The ConsensusPathDB interaction database: 2013 update. Nucleic Acids Res 2013;41:D793–800.
25. Jenssen TK, Laegreid A, Komorowski J, Hovig E. A literature network of human genes for high-throughput analysis of gene expression. Nat Genet 2001;28:21–8.
26. Hosack DA, Dennis GJr, Sherman BT, Lane HC, Lempicki RA. Identifying biological themes within lists of genes with EASE. Genome Biol 2003;4:R70.
27. Huang da W, Sherman BT, Lempicki RA. Systematic and integrative analysis of large gene lists using DAVID bioinformatics resources. Nat Protoc 2009;4:44–57.
28. Griffin GK, Sholl LM, Lindeman NI, Fletcher CD, Hornick JL. Targeted genomic sequencing of follicular dendritic cell sarcoma reveals recurrent alterations in NF-κB regulatory genes. Mod Pathol 2016;29:67–74.
29. Victora GD, Nussenzweig MC. Germinal centers. Annu Rev Immunol 2012;30:429–57.
30. Pardoll DM.The blockade of immune checkpoints in cancer immunotherapy. Nat Rev Cancer 2012;12:252–64.
31. Benson DMJr, Bakan CE, Mishra A, Hofmeister CC, Efebera Y, Becknell B. The PD-1/PD-L1 axis modulates the natural killer cell versus multiple myeloma effect: a therapeutic target for CT-011, a novel monoclonal anti-PD-1 antibody. Blood 2010;116:2286–94.
32. Sage PT, Francisco LM, Carman CV, Sharpe AH. The receptor PD-1 controls follicular regulatory T cells in the lymph nodes and blood. Nat Immunol 2013;14:152–61.
33. Sharpe AH, Wherry EJ, Ahmed R, Freeman GJ. The function of programmed cell death 1 and its ligands in regulating autoimmunity and infection. Nat Immunol 2007;8:239–45.
34. Guarnerio J, Riccardi L, Taulli R, Maeda T, Wang G, Hobbs RM, et al. A genetic platform to model sarcomagenesis from primary adult mesenchymal stem cells. Cancer Discov 2015;5:396–409.
35. Krautler NJ, Kana V, Kranich J, Tian Y, Perera D, Lemm D. , et al. Follicular dendritic cells emerge from ubiquitous perivascular precursors. Cell 2012;150:194–206.
36. Sangaletti S, Tripodo C, Portararo P, Dugo M, Vitali C, Botti L, et al. Stromal niche communalities underscore the contribution of the matricellular protein SPARC to B-cell development and lymphoid malignancies. Oncoimmunology 2014;3:e28989.
37. Hartmann S, Döring C, Agostinelli C, Portscher-Kim SJ, Lonardi S, Lorenzi L, et al. miRNA expression profiling divides follicular dendritic cell sarcomas into two groups, related to fibroblasts and myopericytomas or Castleman's disease. Eur J Cancer 2016;64:159–66.
38. Lu J, Getz G, Miska EA, Alvarez-Saavedra E, Lamb J, Peck D, et al. MicroRNA expression profiles classify human cancers. Nature 2005;435:834–8.

Published OnlineFirst January 27, 2017; DOI: 10.1158/1541-7786.MCR-16-0301




39. Ramaswamy S, Tamayo P, Rifkin R, Mukherjee S, Yeang CH, Angelo M, et al. Multiclass cancer diagnosis using tumor gene expression signatures. Proc Natl Acad Sci U S A 2001;98:15149–54.
40. Crotty S. Follicular helper CD4 T cells (TFH). Annu Rev Immunol 2011;29:621–63.
41. Fazilleau N, Mark L, McHeyzer-Williams LJ, McHeyzer-Williams MG. Follicular helper T cells: lineage and location. Immunity 2009;30: 324–35.
42. Tangye SG, Ma CS, Brink R, Deenick EK. The good, the bad and the ugly - TFH cells in human health and disease. Nat Rev Immunol 2013; 13:412–26.
43. Linterman MA, Pierson W, Lee SK, Kallies A, Kawamoto S, Rayner TF, et al. Foxp3+ follicular regulatory T cells control the germinal center response. Nat Med 2011;17:975–82.
44. Wallin EF, Jolly EC, Suchánek O, Bradley JA, Espéli M, Jayne DR, et al. Human T-follicular helper and T-follicular regulatory cell maintenance is independent of germinal centers. Blood 2014;124:2666–74.
45. Good-Jacobson KL, Szumilas CG, Chen L, Sharpe AH, Tomayko MM, Shlomchik MJ. PD-1 regulates germinal center B cell survival and the formation and affinity of long-lived plasma cells. Nat Immunol 2010; 11:535–42.
46. Gubin MM, Zhang X, Schuster H, Caron E, Ward JP, Noguchi T, et al. Checkpoint blockade cancer immunotherapy targets tumour-specific mutant antigens. Nature 2014;515:577–81.
47. Jacobsen ED, Sharman JP, Oki Y, Advani RH, Winter JN, Bello CM, et al. Brentuximab vedotin demonstrates objective responses in a phase 2 study of relapsed/refractory DLBCL with variable CD30 expression. Blood 2015;125:1394–402.

Published OnlineFirst January 27, 2017; DOI: 10.1158/1541-7786.MCR-16-0301



Molecular Cancer Research

# Distinctive Histogenesis and Immunological Microenvironment Based on Transcriptional Profiles of Follicular Dendritic Cell Sarcomas

Maria Antonella Laginestra, Claudio Tripodo, Claudio Agostinelli, et al.

*Mol Cancer Res* 2017;15:541-552. Published OnlineFirst January 27, 2017.